

RAL 92078
Copy 2 R61 RR
ACCN: 216991

RAL-92-078

Science and Engineering Research Council

Rutherford Appleton Laboratory

Chilton DIDCOT Oxon OX11 0QX

RAL-92-078

***** RAL LIBRARY R61 *****
Acc_No: 216991
Shelf: RAL 92078
R61

Parton Distributions Updated

A D Martin W J Stirling and R G Roberts

LIBRARY, R61
-8 FEB 1993
RUTHERFORD APPLETON
LABORATORY

December 1992

Science and Engineering Research Council

"The Science and Engineering Research Council does not accept any responsibility for loss or damage arising from the use of information contained in any of its reports or in any communication about its tests or investigations"

RAL-92-078
DTP/92/80
November 1992

Parton Distributions Updated

A.D. Martin and W.J. Stirling

*Department of Physics, University of Durham
Durham DH1 3LE, England*

and

R.G. Roberts

*Rutherford Appleton Laboratory,
Chilton, Didcot OX11 0QX, England*

Abstract

We refine our recent determination of parton distributions with the inclusion of the new published sets of precise muon and neutrino deep inelastic data. Deuteron screening effects are incorporated. The $t\bar{t}$ cross section at the FNAL $p\bar{p}$ collider is calculated.

New and very precise data on nucleon structure functions have had a profound impact on our knowledge of parton distributions, especially in the smaller x region. We performed [1] a global structure function analysis which incorporated the preliminary versions of these data which were presented in 1991 [2]. We found that the new measurements led to a significant increase from the previous estimates of the quark distributions for $x \lesssim 0.05$; increases, for example, of more than 30% at $x = 0.01$, $Q^2 = 20 \text{ GeV}^2$. The final form of the new muon and neutrino deep inelastic data have recently been published by the NMC [3] and the CCFR collaboration [4] respectively.

It is necessary to repeat and refine our global analysis [1] for the following reasons.

- (i) Parton distributions play a pivotal role in all hard scattering hadronic processes and the increased precision of the deep inelastic data enables more definitive distributions to be determined.
- (ii) In our previous analysis we treated the preliminary CCFR [4] and the published CDHSW [5] neutrino data with approximately equal weighting. The dramatic improvement in the precision achieved by the CCFR collaboration (and here we incorporate their published errors) mean that the CDHSW measurements play a much reduced role. In fact we omit these latter data from the present fit.
- (iii) We use the published [3], rather than the preliminary [2], NMC data. The differences between the two data sets are in fact small, except at the low Q^2 values of the lower NMC beam energy, which fall outside the cuts ($Q^2 > 5 \text{ GeV}^2$, $W^2 > 10 \text{ GeV}^2$) which we impose on the data fitted in our analysis.
- (iv) The increased precision of the data (coupled with recent theoretical calculations [6,7]) means that screening effects should now be taken into account in extracting the values of $F_2^n(x, Q^2)$ from the NMC measurements [3] of the structure functions for scattering from a deuterium target. We apply the screening corrections calculated by Badelek and Kwiecinski [6], which at most enhance the value of F_2^n by about 2% at the smallest values of x .

The full details of our next-to-leading order analysis can be found in Ref. [1]. There we discuss the other data (BCDMS, EMC deep-inelastic, WA70 prompt photon, and E605 Drell-Yan data) that are simultaneously fitted, the heavy target corrections that are applied, the parametric forms which are used for the parton distributions, and the treatment of the u, d, s, c sea-quark distributions. Following this procedure we are able to update the S_0, D_0 and D_- sets of parton distributions

presented in Ref. [1]. The three new sets, which we denote S'_0 , D'_0 and D'_- , give, as before, equally acceptable descriptions of the data. We note that the "starting" distributions at $Q_0^2 = 4 \text{ GeV}^2$ are required to satisfy $xg, x\bar{q} \sim x^\lambda$ as $x \rightarrow 0$, with $\lambda = 0$ for both S'_0 and D'_0 , and $\lambda = -1/2$ for D'_- . In the S'_0 parametrization \bar{u} and \bar{d} are required to be the *same*, whereas for D'_0 (and D'_-) \bar{u} and \bar{d} are allowed to be *different* with

$$x(\bar{d} - \bar{u}) = A_\Delta x^{\eta_\Delta} (1-x)^{\eta_s} \quad (1)$$

at $Q_0^2 = 4 \text{ GeV}^2$. All three sets are consistent with the same value of Λ of QCD

$$\Lambda_{\overline{\text{MS}}}(n_f = 4) = 230 \pm 55 \text{ MeV}, \quad (2)$$

where the error includes the uncertainty due to scale dependence. This corresponds to

$$\alpha_s(M_Z) = 0.1125^{+0.004}_{-0.005}. \quad (3)$$

The slight increase in the coupling, as compared to Ref. [1], is due to the increased precision of the neutrino data [4] that are fitted.

Figs. 1-4 show the quality of the fit to the various deep-inelastic data. The description of the data is remarkably good (see Table 1), considering the small number of free parameters and the range of processes that are well-described. These include prompt photon production, Drell-Yan and W, Z hadroproduction. The values of the parameters are listed in Table 2. The dashed curves in Fig. 1 show that the predictions of set B_0 of KMRS partons [9] (extrapolated from fits to BCDMS data with $x \gtrsim 0.07$) considerably undershoot the new NMC data at smaller x . This observation is reflected in Fig. 5 which compares the parton distributions of set D'_0 with set B_0 of KMRS at $Q^2 = 20 \text{ GeV}^2$. Though the agreement is excellent for $x \gtrsim 0.1$, we see that the quark distributions differ significantly with decreasing x , reflecting the influence of the new data. It is worth noting that the D'_0 partons are in close agreement with B_0 at $x = 0.1$, whereas the D_0 partons were already different at this x value [1].

The differences between the S_0, D_0, D_- partons (obtained from fits in which the new data were in preliminary form [2]) and the S'_0, D'_0, D'_- sets are small. However the present analysis includes the published errors for the new data. It is therefore more definitive and represents the best that can be done until measurements become available from the experiments at HERA.

There are many applications of the parton distributions. As an example, Table 3 shows some of the key cross sections for the FNAL $p\bar{p}$ collider ($\sqrt{s} = 1.8 \text{ TeV}$).

The W and Z cross sections are computed to $O(\alpha_s^2)$ in the $\overline{\text{MS}}$ scheme with renormalization and factorization scales $\mu = M = M_W$, while the $t\bar{t}$ total cross section is computed to $O(\alpha_s^3)$ for various m_t values with scales $\mu = M = m_t$. The three new sets give very similar predictions and the small differences between them and the previous B_0 predictions can be understood from the differences in the parton distributions shown in Fig. 5. In particular, for the top cross section the slight decrease of a few percent is due to the increase in $\Lambda_{\overline{\text{MS}}}$ and the corresponding steepening of the gluon distribution. The change is in any case much smaller than the estimated overall theoretical uncertainty, which is dominated by the residual scale dependence of the next-to-leading order cross sections. A more complete discussion can be found in Ref. [10].

Acknowledgements

We are grateful to Jan Kwiecinski, Ian Bird and Mike Shaevitz for useful discussions and communications concerning the experimental data.

References

- [1] A.D. Martin, R.G. Roberts and W.J. Stirling, RAL preprint RAL-92-021 (1992), Phys. Rev. (in press).
- [2] Proc. of Joint Int. Lepton-Photon Symposium and Europhysics Conf. on HE Physics, Geneva, July 1991, eds. S. Hegarty, K. Potter and E. Quercigh (World Scientific, 1992), Vol. 1 p. 147 (I. Bird, NMC), p. 135 (S. Mishra, CCFR collaboration).
- [3] NMC collaboration: P. Amaudruz *et al.*, preprint CERN-PPE-92-124 (1992).
- [4] CCFR collaboration: Phys. Rev. Lett., to be published.
- [5] CDHSW collaboration: J.P. Berge *et al.*, Zeit. Phys. **C49** (1990) 187.
- [6] B. Badelek and J. Kwiecinski, Nucl. Phys. **B370** (1992) 278.
- [7] V.R. Zoller, Phys.Lett. **279B** (1992) 145; Zeit. Phys. **C54** (1992) 425.
- [8] BCDMS collaboration: A.C. Benvenuti *et al.*, Phys. Lett. **223B** (1989) 485.
- [9] J. Kwiecinski, A.D. Martin, R.G. Roberts and W.J. Stirling, Phys. Rev. **D42** (1990) 3645.
- [10] A.D. Martin, R.G. Roberts and W.J. Stirling, Phys. Rev. **D43** (1990) 3648.

Table Captions

- [1] Description of the deep inelastic data for the three sets of partons shown in terms of χ^2 .
- [2] The upper portion of the table lists the values of the parameters of the parton distributions as defined in [1] found in the three types of optimum fit to the data. For sets S'_0 and D'_0 we fix the gluon exponent $\lambda = 0$, and for D'_- we set $\lambda = -\frac{1}{2}$. We also list the value of the Gottfried sum rule I_{GSR} . Finally, we show the values of the ($O(\alpha_s^2)$) K' factor [1] which are required to achieve agreement with the Drell-Yan data of E605.
- [3] Cross sections for W , Z and $t\bar{t}$ production in $p\bar{p}$ collisions at $\sqrt{s} = 1.8$ TeV. Leptonic branching ratios are included for the former. For the latter, the number given in brackets is m_t in GeV.

Expt.		No. of data	χ^2		
			S'_0	D'_0	D'_-
BCDMS	$F_2^{\mu p}$	142	144	153	158
NMC	$F_2^{\mu p}$	74	96	96	98
NMC	$F_2^{\mu D}$	74	74	74	70
EMC	F_2^n/F_2^p	10	3	3	3
BCDMS	F_2^n/F_2^p	11	6	4	4
NMC	F_2^n/F_2^p	11	21	15	15
CCFR	$F_2^{\nu N}$	77	46	53	50
CCFR	$x F_3^{\nu N}$	77	19	19	20

Table 1

	S'_0	D'_0	D'_-
$\Lambda_{\overline{MS}}^{(4)}$ (MeV)	230	230	230
Glue			
λ	0	0	-0.5
γ_g	0	0	10.6
A_g	2.78	2.78	0.338
η_g	5.3	5.3	5.3
Valence			
η_1	0.31	0.42	0.42
η_2	3.85	3.92	3.92
η_3	0.82	0.24	0.24
η_4	4.60	4.67	4.67
ϵ_{ud}	6.12	2.31	2.59
γ_{ud}	9.86	4.43	4.21
ϵ_d	-1.38	43.3	28.7
γ_d	1.10	7.62	8.58
Sea			
η_S	10	10	7.4
A_S	1.98	2.03	0.083
γ_S	7.98	8.47	15.8
ϵ_S	-2.68	-2.98	8.57
A_Δ	0	0.152	0.164
η_Δ	-	0.42	0.42
D-Y K' factor	1.10	1.08	1.06
I_{GSR}	0.333	0.256	0.240

Table 2

σ (pb)	B_0	S'_0	D'_0	D'_-
$B\sigma_W$	2090	2420	2420	2390
$B\sigma_Z$	200	225	226	223
$\sigma_{t\bar{t}}$ (110)	58.0	55.9	56.2	53.7
$\sigma_{t\bar{t}}$ (120)	36.9	35.7	35.9	34.7
$\sigma_{t\bar{t}}$ (130)	24.2	23.5	23.7	23.1
$\sigma_{t\bar{t}}$ (140)	16.4	16.0	16.0	15.7
$\sigma_{t\bar{t}}$ (150)	11.3	11.1	11.1	11.0
$\sigma_{t\bar{t}}$ (160)	7.97	7.83	7.85	7.79

Table 3

Figure Captions

- [1] The continuous curves show the description of the BCDMS [8] and NMC [3] measurements of the $F_2^{\mu p}(x, Q^2)$ structure function by the D'_0 set of partons. The dashed curves show the predictions obtained from the KMRS (set B_0) parton distributions [9]. For $x \gtrsim 0.1$ the dashed and continuous curves are essentially identical. The statistical and systematic errors of the data have been combined in quadrature.
- [2] The description of the NMC data [3] for the structure function ratio $F_2^{\mu n} / F_2^{\mu p}$ given by the S'_0 , D'_0 and D'_- sets of parton distributions. The mean Q^2 of the data varies with x as shown by the uppermost scale. The curves take this Q^2 dependence into account. The values of $F_2^{\mu n}$ have been obtained from μD data corrected for deuteron screening effects [6].
- [3] The continuous curves show the description of the CCFR [4] measurements of the $F_2^{\nu N}(x, Q^2)$ structure function by the D'_0 set of partons. The data are shown after correction for the heavy target effects and after the overall renormalization of 0.95 required by the global fit. The statistical and systematic errors of the data have been combined in quadrature.
- [4] As for Fig. 3 but for the structure function $x F_3^{\nu N}(x, Q^2)$.
- [5] The parton distributions for the u , d , s quarks and the gluon at $Q^2 = 20 \text{ GeV}^2$ obtained in the D'_0 fit (continuous curves) compared with the earlier KMRS(B_0) distributions [9] (dashed curves).

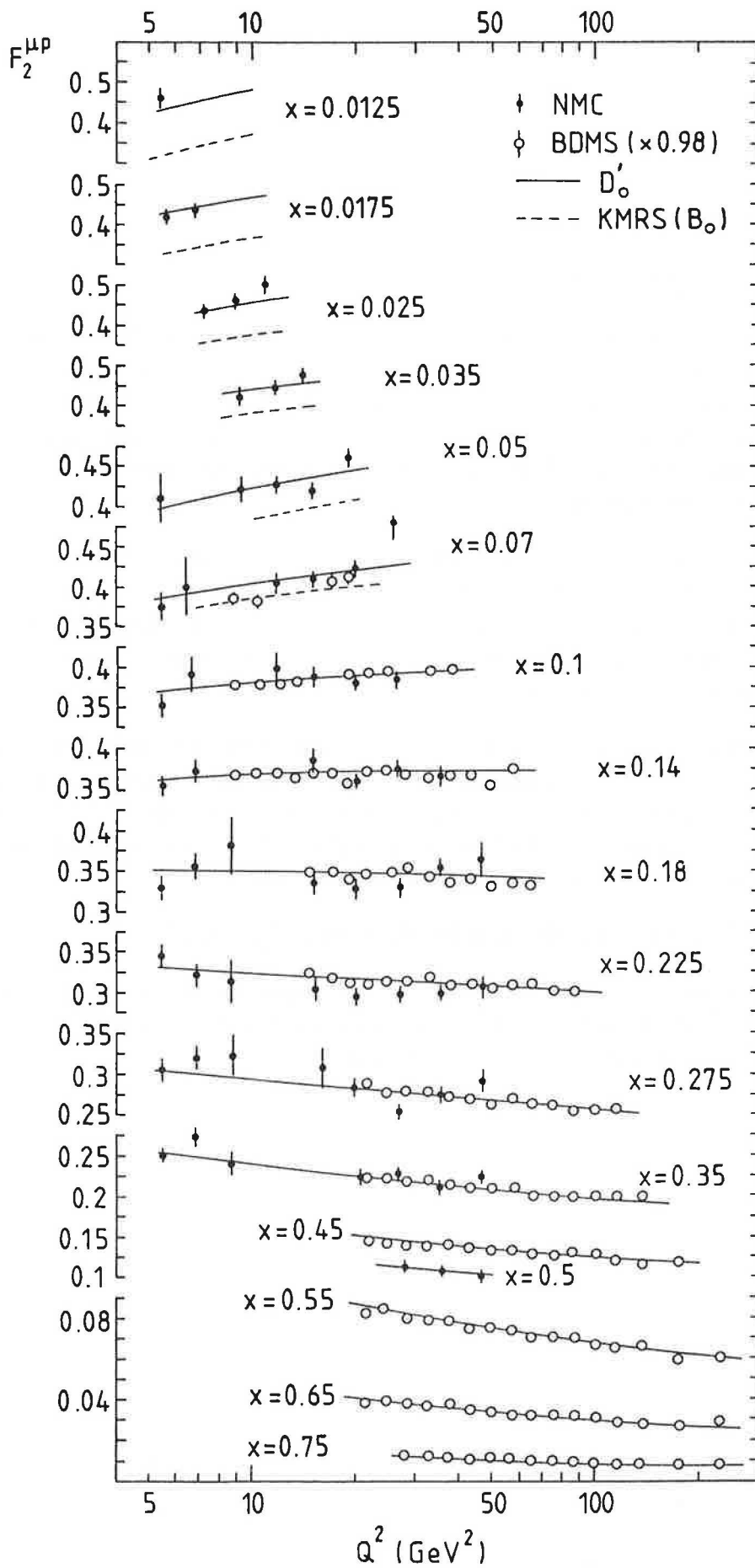


Fig. 1

Fig.1

Fig. 2

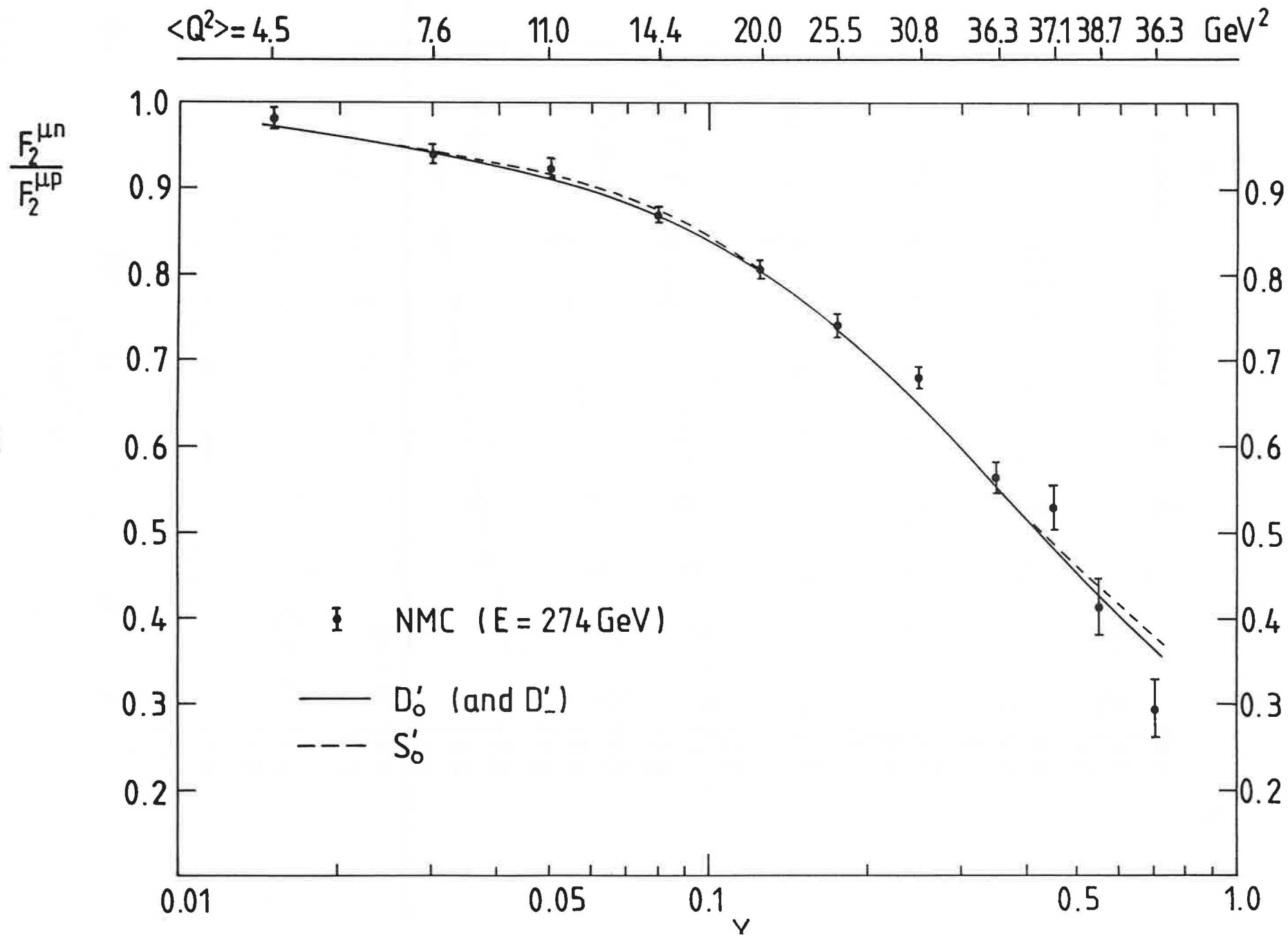


Fig. 2

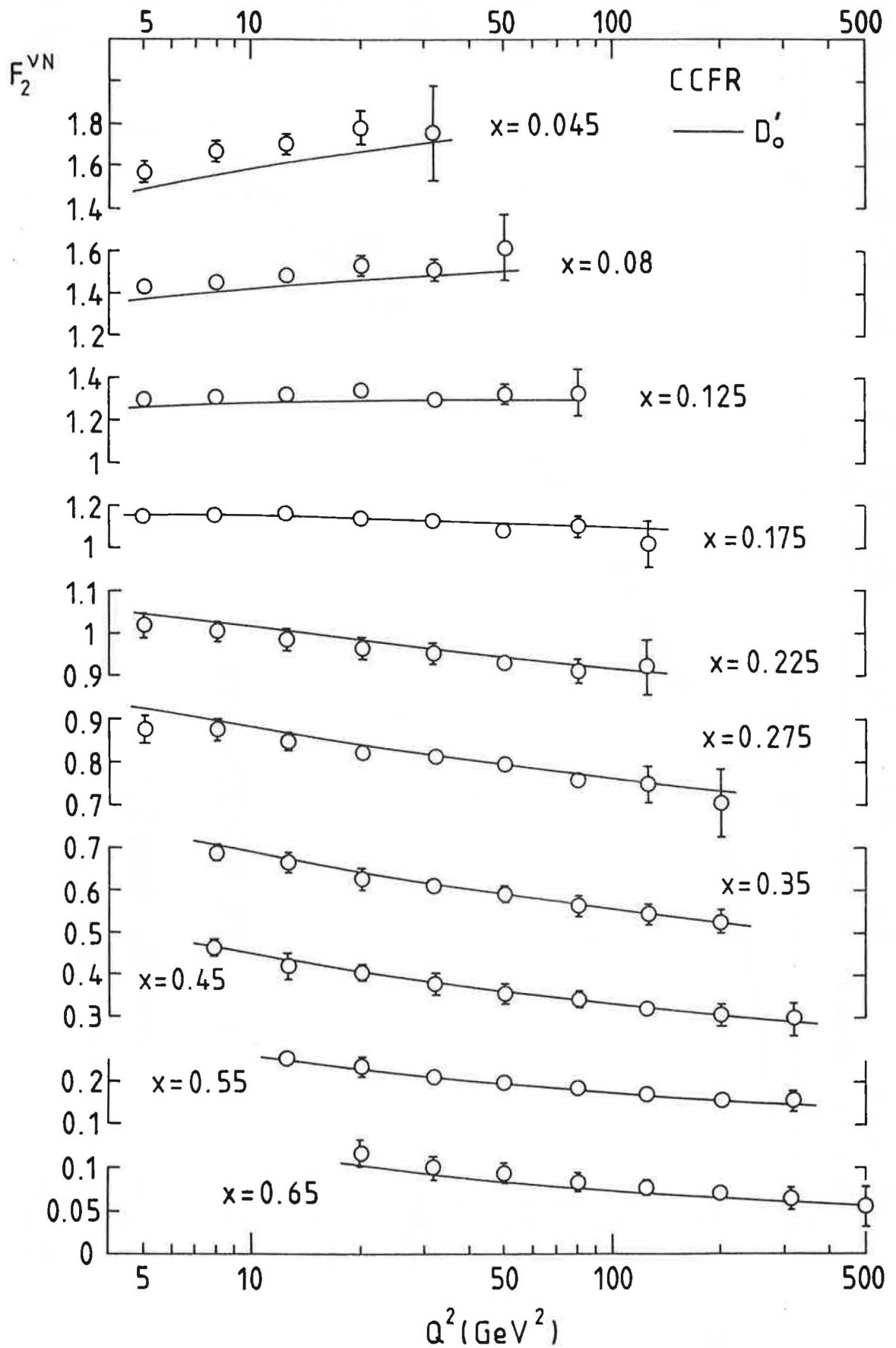


Fig. 3

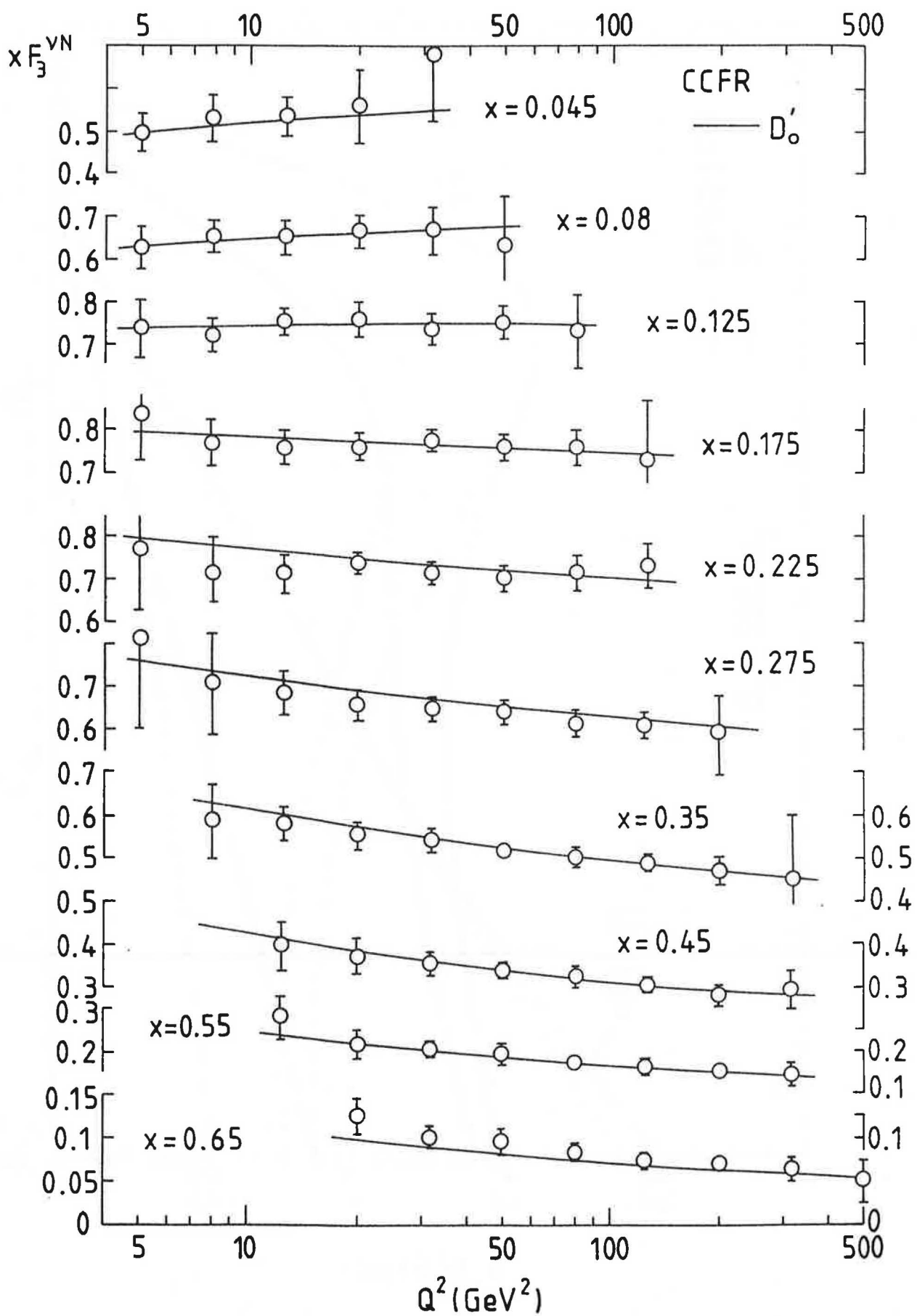


Fig. 4

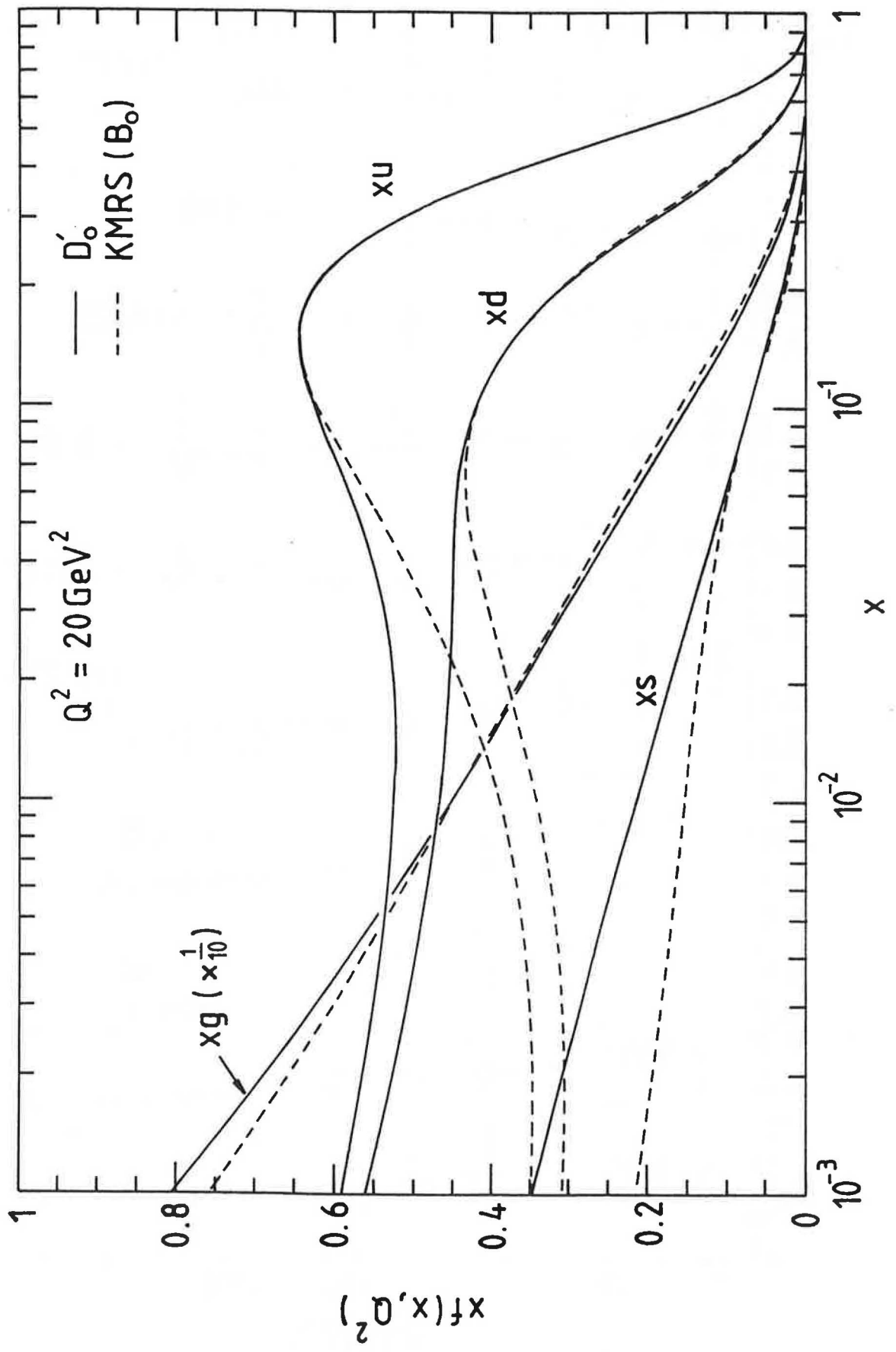


Fig.5

